

AN EXPERIMENTAL TESTBED OF MULTI-AGENT SYSTEM FOR CAMPUS BUILDING ENERGY MANAGEMENT USING EMBEDDED PLATFORM AND SCADA SYSTEM

ARYUANTO SOETEDJO, IRRINE BUDI SULISTIAWATI
AND RADIMAS PUTRA MUHAMMAD DAVI LABIB

Department of Electrical Engineering
National Institute of Technology (ITN) Malang
Jln. Raya Karanglo Km.2, Malang, Jawa Timur 65143, Indonesia
{aryuanto; irrine; radimas}@lecturer.itn.ac.id

Received September 2024; revised December 2024

ABSTRACT. *The building energy management system (BEMS) is a system that manages the energy efficiency of a building. It is a part of the Smart Grid system, a modern electricity technology. This paper proposes a campus building energy management based on the multi-agent system (MAS). The proposed MAS is evaluated on a testbed that combines the embedded platform and supervisory control and data acquisition (SCADA). It introduces the optimizer agent to handle the optimization task, the predictor agent to predict the photovoltaic (PV) power, the user interface agent to monitor and control the system, and the other agents related to the occupancy and electrical load control. The artificial intelligent (AI) algorithms are adopted in the agents, namely the genetic algorithm (GA) for optimization and long short-term memory (LSTM) for prediction. The experimental results show that the proposed testbed performs effectively for real-time MAS-based energy management system simulation. The simulation using five days' real dataset shows that the Occupancy and Temperature Control method achieves an energy consumption reduction by 40.29%. Furthermore, the SCADA human machine interface (HMI) provides valuable monitoring and control of the MAS, which can easily be deployed for real applications.*

Keywords: Multi-agent system, Energy management, Embedded system, SCADA, Intelligent system

1. Introduction. Smart Grid, a modern electricity technology, is a vital infrastructure to overcome climate change and energy crisis problems [1]. It offers an efficient way to produce, deliver, and consume energy. In the energy consumption part, the energy management system (EMS) is required to efficiently manage the energy consumption in the office and campus buildings, industry, and home [2]. A typical EMS consisted of the sensing and measurement units, actuator devices, processing engine, and user interfaces. The processing engine performed the optimization tasks using a rule-based algorithm or machine learning techniques. The user interface was used to interact with the user such as displaying the energy consumption or setting the user preferences.

The EMS implementation should consider three main factors [3,4]: a) Integration of several energy resources and loads; b) Intelligence, i.e., the real-time decision to respond to the data; c) Scalability and autonomy, that is referred to the ability to adapt the changes of the supply and demand. Considering the first factor, the integration of the electricity grid and renewable energy, such as photovoltaic (PV), is a common approach in the EMS [5-8]. The second factor is related to the processing engine as described before.

It is common to adopt the artificial intelligence (AI) techniques, such as artificial neural networks (ANN) for predicting the energy demand [5], optimization (energy consumption, electricity cost) [9]; fuzzy logic for cost reduction by intelligent selection of energy resources [6], load scheduling [10], energy consumption recommendation from environmental data [11]; genetic algorithm (GA) for cost reduction [12]; particle swarm optimization (PSO) for load shifting [7].

The increasing demand for electricity and power system complexity cause the inefficiency of the centralized system. Thus, it led to the decentralized concept, namely the multi-agent system (MAS) [13]. A MAS involves multiple intelligent agents collaborating to solve problems [14]. It can be used to solve the complex and non-linear problem such as the containment control system, where there are followers and leaders agents [15]. The MAS has been adopted for energy management systems in the micro-grid [16,17], smart grid [18,19], smart home [20-23], smart building [24-32].

Due to the complexity and large size of MAS-based building energy management systems, most researchers conduct simulations or prototypes to evaluate their proposed systems. In [25], the prototype of MAS was implemented on the embedded systems. It consisted of a sensor, actuator, management, and user interface agents. The sensor agent was used to sense the ambient light, temperature, window/door opening, and occupancy. The actuator agent was used to activate the lighting and heating units. The management agent performed the decision-making algorithm to minimize energy consumption while maximizing user comfort. The user interface agent is used for visualization and manual control. The Modbus protocol was adopted to communicate between agents via Ethernet, serial RS485, and Zigbee.

The MATLAB simulation of MAS for energy management in the classrooms was proposed in [26], where it consisted of the load, photovoltaic (PV), grid, and central control agents. The load agents control the lamps, LCD projector, and air conditioner (AC) in a classroom based on the occupancy, outdoor temperature, and the availability of PV source. The load agent determined the AC temperature setpoint using the fuzzy logic controller. The central control agent adopted the fuzzy logic controller to minimize the electricity cost by maximizing the PV usage.

The hardware testbed of extended work of [26] was developed in [27], where the MAS was implemented on the embedded platform. Instead of the fuzzy logic controller for implementing the energy management algorithm, the central control agent on a Raspberry single-board computer adopted the GA for optimizing energy consumption in the classroom, laboratory, and office. The optimization objective was similar to [25], i.e., minimizing the power consumption while maintaining the user comfort (room temperature and lighting intensity). The load agent was implemented on a microcontroller communicating with the load simulator using Modbus TCP via WiFi and connected to the central control agent using MQTT protocol.

In [28], the MAS simulation was developed to manage the energy in the residential green building integrated with distributed energy resources. It consisted of the generation agent that monitored and defined a setpoint to balance the generation and demand load, the demand response agent that controlled the loads (load shedding) during peak hours, the energy storage agent that managed the energy storage for load balancing between supply and demand, the neighborhood system operator agent that provided the data of generation and consumed power, and the central neighborhood system operator agent that optimized the price bids and defined the power should be supplied by the neighborhood system operator.

The MATLAB simulation of MAS for energy-efficient building was proposed in [31]. It consisted of the local temperature, lighting, and air quality agents for measuring the

temperature, light intensity, and air quality, respectively, and the control agent that performed the optimization by maximizing the comfort level and minimizing the energy consumption. There were two optimization methods. The first method, a constrained nonlinear optimization, optimized the temperature, lighting intensity, and air quality parameters. The second method was the selection of a set of optimized solutions using the artificial neural network.

A fog building energy management system (Fog BEMS) prototype testbed was developed in [32]. The fog architecture was adopted to handle the increase in end devices in the BEMS. In this system, a MAS concept was used in the programming model of the node. A fog node can be categorized as a sensing agent that collects the sensors' data, an action agent that controls the loads, and a user agent for user interfacing. This memory agent manages the local database, an intelligent agent that performs data analyses and decisions, a communication agent for connecting other fog nodes and agents, an Internet agent for collecting data via the Internet (weather data, time of use price), and an application agent for handling specific functions. The sensing and action agents communicate directly with the end devices using Modbus TCP, XML, or JSON protocols. The intelligent agent performed two rules: set the lighting brightness based on the light sensor and define the AC temperature setpoint based on the electricity price.

The current implementation of EMS in the building faces several challenges in the optimization algorithms and hardware integration. The implemented EMS usually uses a simple, rule-based technique that fails to achieve optimal energy efficiency [33]. There is no standard communication protocol for the hardware infrastructure in the building, and different manufacturers use different protocols [33-35]. To overcome these issues, we propose the MAS-based EMS that adopts the GA technique for optimizing the building energy consumption using the Internet of Things (IoT)-based supervisory control and data acquisition (SCADA) system. The proposed GA is implemented on an embedded platform that allows the algorithm to be implemented on the actual building. The IoT-based SCADA is selected due to the benefits of the SCADA user-friendly interface and the IoT protocol standardization for easy integration with the existing devices.

The proposed MAS-based EMS deals with the campus building for the following reasons. Campus buildings have different characteristics than other buildings, such as offices or factories. Occupancy in campus buildings is uncontrolled [36]. The occupant activities are dominated by teaching and research activities in the classrooms and laboratories, where occupancy time is not determined strictly, unlike in the office or factory. For instance, the classrooms may be fully occupied from the morning to afternoon, half-day occupied, or not occupied during the day. In contrast, most room or building occupancy in an office or factory is determined properly by the staff's working time. A campus building tends to cause energy waste when no advanced building control is adopted [7]. Therefore, implementing an energy management system in a campus building is exciting and challenging.

As described previously, the simulation or hardware prototype is usually used by the researchers to test the proposed EMS. Compared to the hardware prototype, the simulation software offers a straightforward implementation, especially for complex algorithms. However, it does not reflect the actual conditions. On the contrary, the hardware prototype better represents the actual condition, especially in terms of real-time processing and actual application. Therefore, this paper presents the hardware testbed for implementing the MAS-based campus building energy management system.

In this work, for simplicity and without loss of generality, the proposed system deals with energy management in different buildings in a campus, namely classrooms, office

rooms, and laboratories. The rooms are selected due to the different occupancy and energy usage characteristics as described previously.

The main contributions of the proposed system are as follows.

- 1) The proposed MAS adopts AI-based techniques, namely long short-term memory (LSTM) for PV power prediction and GA for optimization, in the sense that the algorithm runs in real time.
- 2) It combines the embedded platform and IoT-based SCADA system for real-time implementation. This approach exploits the benefits of an embedded platform for real-time implementation of the proposed AI-based algorithms, the superiority of the SCADA system for monitoring and control tasks, and the standardization of IoT protocol.

The rest of this paper is organized as follows. Section 2 describes the proposed system. Section 3 presents the results and discussion. Conclusions are covered in Section 4.

2. Proposed System.

2.1. MAS architecture. The proposed MAS is depicted in Figure 1. It consists of six agents: power source agent (PSA), occupancy-based load control agent (OLA), temperature-based load control agent (TLA), supervisory and monitoring agent (SMA), optimizer agent (OA), and predictor agent (PA). The PSA is an agent used to manage power sources, i.e., utility grids and PV plants. In this work, the grid-connected PV system is used as the electrical power source in the campus building. The PSA communicates with the SMA for sending the power generation data.

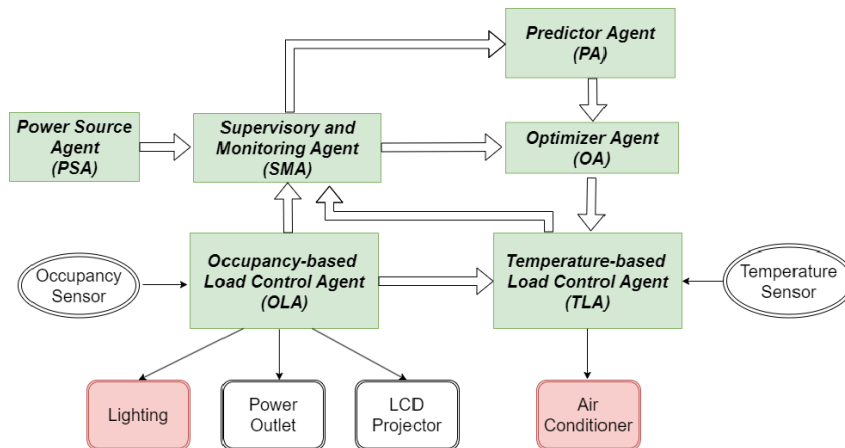


FIGURE 1. MAS architecture

The OLA and TLA are the agents that control the loads. Instead of using the load agent on a specific load, we use the load agent based on a specific control method, namely occupancy-based and temperature-based control. The OLA is an agent that handles occupancy-based load control. The occupancy-based loads are the loads that are controlled (switched on/off) based on the occupancy. As shown in Figure 1, the loads consist of lighting, power outlet, and LCD projector. They are the typical loads used in the classroom, office, and laboratory rooms. The loads are operated when there is an occupant, which is sensed by the occupant sensor, in the room. The OLA sends the load power and occupancy data to the SMA. The occupancy data is also sent to the TLA to activate the air conditioner (AC).

The TLA is an agent that handles temperature-based load control. In this case, it deals with AC operation, i.e., turning on/off based on occupancy and setting the temperature according to the optimal setpoint received from the OA. By determining the

optimal temperature, the AC consumption can be optimized. The TLA receives the room temperature from the temperature sensor and sends the data to the SMA. The TLA also sends the AC power consumption data to the SMA.

The PA is an agent used to predict PV power generation. It predicts PV power generation based on previous PV power data received from the SMA. The predicted PV power is then sent to the OA for optimization. The prediction algorithm is explained in the next section.

The OA is an agent that performs the optimization task. It optimizes the AC temperature setpoint based on the PV power, consumed power, and room temperature. The TLA receives the consumed power and the room temperature data from the SMA, and PV power generation data from the PA. The optimization algorithm is explained in the next section.

Compared to the existing approaches, our proposed MAS offers two benefits. First, it adopts the IoT-based SCADA system as the SMA. Since SCADA is an established monitoring system commonly used in industry, our proposed MAS can be integrated and expanded with existing devices easily. Second, the combination of optimization (OA) and prediction (PA) provides a better optimization process because the OA optimizes the temperature setpoint based on the predicted PV power data in the future.

2.2. Hardware configuration. The configuration of the proposed hardware testbed is illustrated in Figure 2. The testbed is mainly dedicated to implementing the optimization and prediction algorithms on the embedded platform and the supervising and monitoring process on the SCADA HMI. Rather than implementing the electrical parts on the devices,

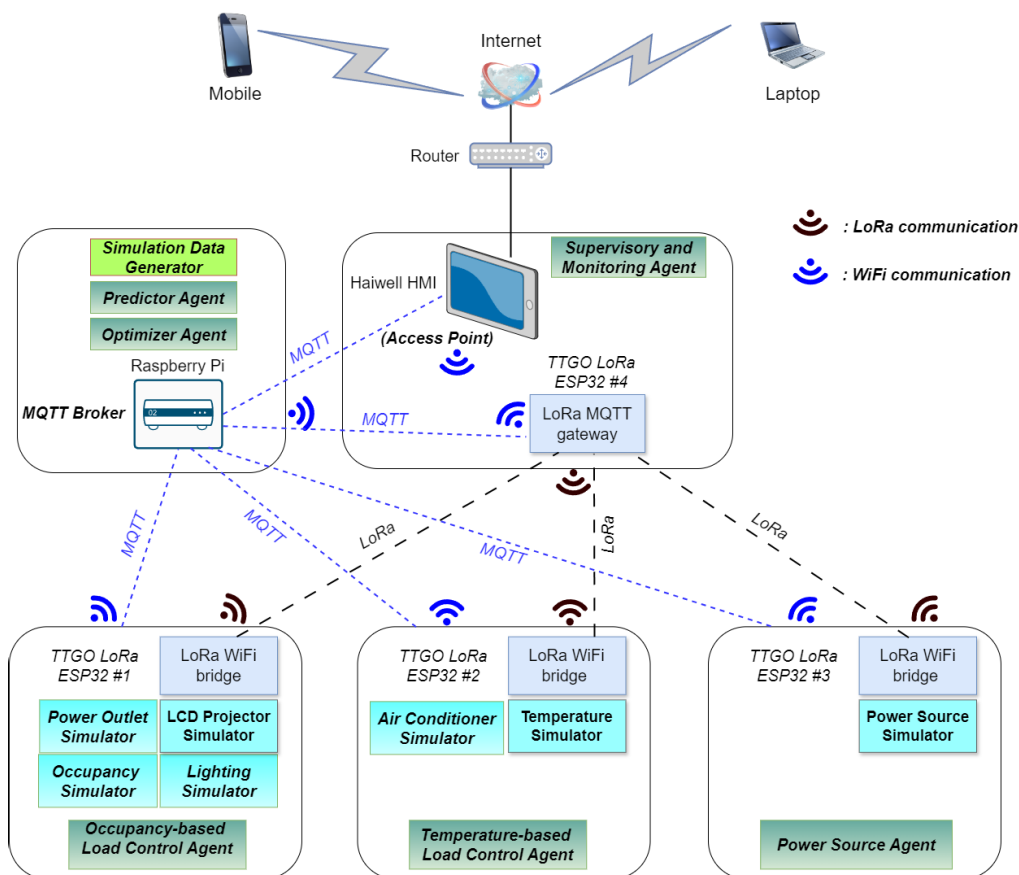


FIGURE 2. (color online) Hardware configuration

they are simulated on the embedded system. The testbed shown in Figure 2 consists of three primary devices: TTGO LoRa ESP32 microcontroller system, Raspberry Pi single-board computer, and Haiwell HMI.

As shown in Figure 2, there are two wireless communication protocols: WiFi and LoRa. WiFi is used to communicate between devices in a room or between rooms in a building. Meanwhile, LoRa is used for long-range communication between campus buildings. Fortunately, both WiFi and LoRa communication modules are supported by the TTGO LoRa ESP32. Therefore, data communication between agents in the same building or with different buildings can be carried out effectively.

The TTGO LoRa ESP32 is an ESP32-based development module incorporating LoRa communication. The specification is given in Table 1. This work uses the TTGO LoRa ESP32 to implement the OLA, TLA, PSA, load, temperature simulators, LoRa module, and LoRa MQTT gateway. As the agent (OLA, TLA, PSA), the device communicates with the SMA via the LoRa module. In this case, the LoRa MQTT gateway is required to exchange the LoRa protocol for the MQTT protocol used by the SMA (Haiwell HMI). It benefits from the valuable tool provided by the OpenMQTTGateway [37]. As the simulator (Power Outlet (POS), LCD Projector (LPS), Occupancy (OSS), Lighting (LGS), AC (ACS), Temperature (TMS), and Power Source (PSS)), the device communicates with the simulation data generator (SDG) via WiFi communication using MQTT protocol.

TABLE 1. Specification of TTGO LoRa ESP32

Item	Specification
A. ESP32	
Chip	Xtensa dual-core 32-bit LX6 microprocessor, up to 240MHz
ROM	448 KB
SRAM	520 KB
B. WiFi	
Protocol	802.11 b/g/n
Frequency range	2.4GHz ~ 2.5GHz
C. LoRa	
Chip	SX1276
Operating frequency	915MHz
Transmission power	+20dBm

The Raspberry Pi 5 is a single-board computer with the specification given in Table 2. The Raspberry Pi implements the PA, OA, SDG, and MQTT broker. As the OA, the Raspberry Pi communicates with the SMA using the MQTT protocol and TLA using MQTT and LoRa protocols (via LoRa MQTT gateway). As the PA, it communicates with the SMA using the MQTT protocol. As the SDG, it communicates with the simulator (TTGO LoRa ESP32) using the MQTT protocol. Since the MQTT protocol requires the MQTT broker, it is implemented on the Raspberry Pi 5. The MQTT protocol defines

TABLE 2. Specification of Raspberry Pi 5

Item	Specification
Processor	Broadcom BCM2712 2.4GHz quad-core 64-bit Arm Cortex-A76 CPU
SDRAM	2GB, 4GB and 8GB
WiFi	Dual-band 802.11ac
Ethernet	Gigabit Ethernet, with PoE+ support

TABLE 3. MQTT topics

MQTT topic	Publisher	Subscriber	Remark
cmd/MASBEMS/ LORAtoMQTT/123	OLA TLA PSA	SMA PA OA	Data exchange between agents: sent by OLA, TLA, PSA
cmd/MASBEMS/ predictiondata/123	PA	OA SMA	Data exchange between agents: sent by PA (Prediction data)
cmd/MASBEMS/ commands/MQTTtoLORA	OA	TLA	Data exchange between agents: sent by OA (Optimization data)
sim/data1	SDG	OSS LGS LPS POS	Data exchange for simulation: sent by SDG
sim/data2	SDG	ACS TMS	
sim/data3	SDG	PSS	

TABLE 4. Specification of Haiwell HMI

Item	Specification
Screen size	10.1" TFT
Resolution	1280 × 800 pixels
Touch panel type	Analog resistive film
Flash memory	4GB
RAM	1GB
Ethernet port	10/100 Base-T; 10/100/1000 Base-T
WiFi	802.11b/g/n
Programming software	Haiwell Cloud SCADA

the messages according to the topics listed in Table 3. It is noted here that the messages for the simulation process, which the SDG publishes, are separated from the agent tasks. Thus, the proposed system can be easily deployed for actual application by replacing the simulator part without changing the agent parts.

The Haiwell HMI is the IoT-based SCADA HMI system, as specified in Table 4. It is commonly used in the industrial automation system. In this work, the Haiwell HMI is the SMA and the WiFi access point for all WiFi devices used in the experiments. The device is equipped with the MQTT protocol for interfacing with the other IoT-enabled devices. Further, it is connected to the cloud server for remote access via the Internet. The HMI is programmed using the Haiwell Cloud SCADA software, equipped with the user interface designer tool to develop a user-friendly graphical interface quickly.

2.3. Optimization and prediction techniques. The objective of the proposed campus building energy management is to minimize the load energy consumption by optimizing the temperature setpoint of the AC, while maintaining the user comfort. The objective functions are expressed as

$$\text{Maximize} \left(\frac{CT_{\max} - CT_{\text{opt}}}{CT_{\max} - CT_{\min}} \right)^2 \quad (1)$$

$$\text{Maximize} \left(\frac{LT_{\max} - LT_{opt}}{LT_{\max} - LT_{\min}} \right)^2 \quad (2)$$

$$\text{Maximize} \left(\frac{OT_{\max} - OT_{opt}}{OT_{\max} - OT_{\min}} \right)^2 \quad (3)$$

$$\text{Maximize} (PPV - P_T (CT_{cur} - CT_{opt}) - P_T (LT_{cur} - LT_{opt}) - P_T (OT_{cur} - OT_{opt}) - PLG - PPO - PLP) \quad (4)$$

$$\text{Subject to } P_T (CT_{cur} - CT_{\max}) \leq P_T (CT_{cur} - CT_{opt}) \leq P_T (CT_{cur} - CT_{\min}) \quad (5)$$

$$P_T (LT_{cur} - LT_{\max}) \leq P_T (LT_{cur} - LT_{opt}) \leq P_T (LT_{cur} - LT_{\min}) \quad (6)$$

$$P_T (OT_{cur} - OT_{\max}) \leq P_T (OT_{cur} - OT_{opt}) \leq P_T (OT_{cur} - OT_{\min}) \quad (7)$$

$$CT_{\min} \leq CT_{opt} \leq CT_{\max} \quad (8)$$

$$LT_{\min} \leq LT_{opt} \leq LT_{\max} \quad (9)$$

$$OT_{\min} \leq OT_{opt} \leq OT_{\max} \quad (10)$$

$$CT_{\max} \leq CT_{cur} \quad (11)$$

$$LT_{\max} \leq LT_{cur} \quad (12)$$

$$OT_{\max} \leq OT_{cur} \quad (13)$$

$$P_T (CT_{cur} - CT_{opt}) + P_T (LT_{cur} - LT_{opt}) + P_T (OT_{cur} - OT_{opt}) + PLG + PPO + PLP \leq Grid_{tot} \quad (14)$$

where

PLG : Power consumption of lighting

PPO : Power consumption of power outlet

PLP : Power consumption of LCD projector

PPV : Power generated by PV

$Grid_{tot}$: Maximum Grid power

P_T = Required power to change the temperature per degree Celcius (80 Watt/°C)

CT_{opt} = Optimized temperature of classroom

CT_{cur} = Current temperature of classroom

CT_{\min} = Minimum temperature setpoint of classroom (20°C)

CT_{\max} = Maximum temperature setpoint of classroom (24°C)

LT_{opt} = Optimized temperature of laboratory room

LT_{cur} = Current temperature of laboratory room

LT_{\min} = Minimum temperature setpoint of laboratory room (20°C)

LT_{\max} = Maximum temperature setpoint of laboratory room (24°C)

OT_{opt} = Optimized temperature of office room

OT_{cur} = Current temperature of office room

OT_{\min} = Minimum temperature setpoint of office room (20°C)

OT_{\max} = Maximum temperature setpoint of office room (24°C)

Equations (1), (2), and (3) represent the maximization of the temperature comfort index in the classroom, laboratory room, and office room, respectively. Equation (4) represents the maximization of the PV power usage consumed by the loads. Equation (4) will be maximized when the consumed power is minimized. Thus, Equations (1) to (4) reflect the objection function as defined previously, i.e., minimizing the power consumption while maintaining the temperature comfort index. The multi-objective optimization problems with the constraints expressed by Equations (1) to (14) are solved using the multi-objective genetic algorithm (MOGA) as adopted in [27]. The MOGA is implemented using the Python language and Platypus library [38].

The MOGA in [27] is implemented on the Raspberry Pi 3 Model B, which needs about 14 seconds to run the algorithm. Thus, the resulting optimized parameters are not relevant to the parameters in the time ahead. It is a common problem in the real-time control. The prediction value can be used instead of the current value to overcome this drawback. Therefore, in this work, we propose the prediction technique using the LSTM to predict the PV power generation, where the optimization algorithm then uses the predicted value. Compared to the existing works that adopt LSTM for PV prediction using offline data [39-41], our approach runs the algorithm in a real-time manner. It takes the benefit of the Raspberry Pi single-board computer that provides an effective solution for a real-time application. The LSTM is implemented using Python, TensorFlow, and Keras.

3. Results and Discussion. Several experiments are conducted to evaluate the proposed system using a real dataset simulated in real time. The datasets contain data on PV power generation, occupancy, and room temperature over five days (Monday to Friday) at five-minute intervals. The dataset on PV power generation is used by the predictor agent (PA) to predict PV power in the next five-minute intervals using the LSTM algorithm. The dataset consists of three tables: PV power, PV temperature, and solar irradiation. It contains 4320 data in three tables, with 1440 data on each table. The occupancy and room temperature datasets consist of seven tables in each dataset: Classroom #1, Classroom #2, Classroom #3, Classroom #4, Office room, Laboratory room #1, and Laboratory room #2. Each table contains 1440 data that simulates the five-minute interval data during five days.

In the experiments, the five-minute time interval of the real dataset is simulated in a four-second time interval. Therefore, 90 minutes is required to complete a dataset (1440 data points). The room usage time table in Table 5 represents the occupancy data. The load power ratings in the rooms are given in Table 6. As shown in Table 7, four load control methods are used in the evaluation.

3.1. HMI monitoring system. The proposed HMI main display is depicted in Figure 3. The layout of the classroom, office room, and laboratory room are shown in the figure, with the occupancy status (indicated by a red circle) and the values of load power consumption and room temperature written on the blue box. The panel on the left-upper

TABLE 5. Room usage time table

Room	Monday	Tuesday	Wednesday	Thursday	Friday
Classroom #1	07:00-09:00 10:00-14:00	08:00-12:00 15:00-17:00	07:00-15:00	09:00-11:00 15:00-17:00	07:00-10:00 14:00-16:00
Classroom #2	07:00-09:00 10:00-12:00	08:00-12:00	07:00-12:00	09:00-11:00 15:00-17:00	07:00-10:00 14:00-16:00
Classroom #3	07:00-09:00 10:00-12:00	08:00-12:00	07:00-12:00	15:00-17:00	14:00-16:00
Classroom #4	07:00-09:00 10:00-14:00	10:00-12:00	07:00-12:00	09:00-11:00	07:00-10:00 14:00-16:00
Office room	08:00-12:00 13:00-16:00	08:00-12:00 13:00-16:00	08:00-12:00 13:00-16:00	08:00-12:00 13:00-16:00	08:00-11:30 13:00-16:00
Laboratory room #1	09:00-12:00 13:00-15:00	10:00-12:00 13:00-15:00	09:00-11:00	08:00-12:00 13:00-15:00	08:00-11:00
Laboratory room #2	09:00-12:00 13:00-17:00	09:00-12:00 13:00-17:00	09:00-12:00 13:00-17:00	09:00-12:00 13:00-17:00	09:00-11:30 13:00-17:00

TABLE 6. Loads power rating

Room	Lighting	LCD projector	Power outlet
Classroom #1	60 W	200 W	80 W
Classroom #2	60 W		
Classroom #3	60 W		
Classroom #4	60 W		
Office room	120 W	NA	120 W
Laboratory room #1	240 W	200 W	100 W
Laboratory room #2	60 W		400 W

TABLE 7. Load control method

Method	Remark
No Control	Load operation time is fixed AC temperature setpoint is fixed
Temperature Control	Load operation time is fixed AC temperature setpoint is based on optimized control
Occupancy Control	Load operation time is based on occupancy AC temperature setpoint is fixed
Occupancy and Temperature Control	Load operation time is based on occupancy AC temperature setpoint is based on optimized control

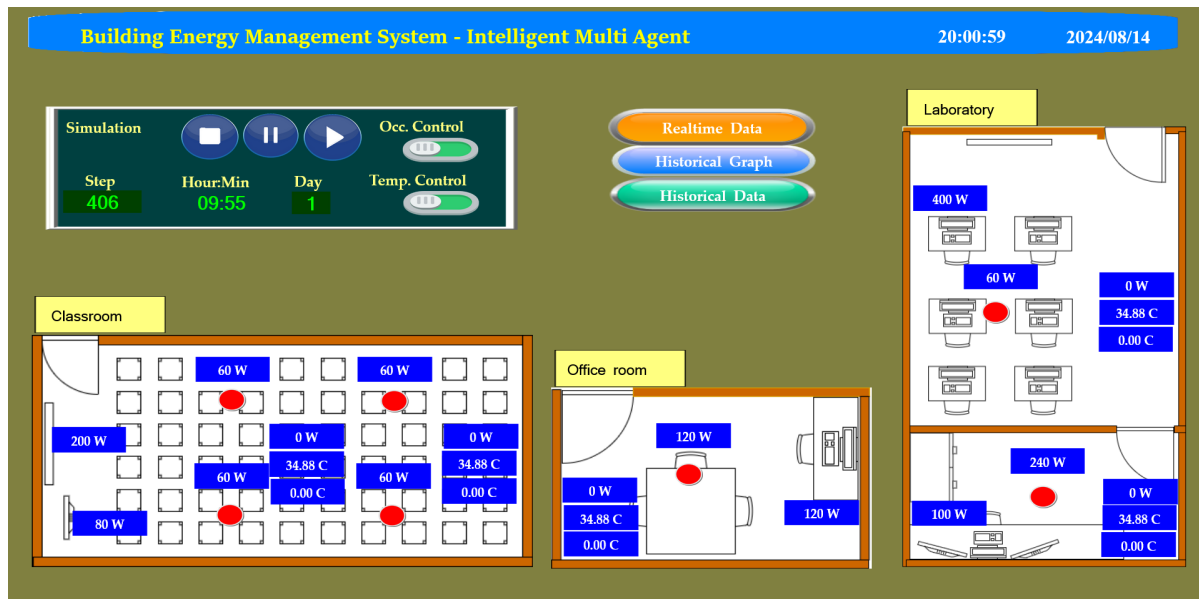


FIGURE 3. HMI main display

part is the simulation panel used to start the simulation and monitor the time step of the simulation process. It is also equipped with buttons to select the load operation control, i.e., Occupancy and Temperature Control methods. The buttons on the middle-upper side can be used to select the real-time data, historical graph, and historical data menus.

The real-time data monitoring display is depicted in Figure 4. The information about the agents is shown in the figure. The OLA panel shows the occupancy sensor status, lighting power and energy, LCD projector power and energy, and outlet power and energy. The TLA panel shows the room, optimized temperature, AC power, and energy. The PSA



FIGURE 4. HMI data monitoring display

panel shows the PV power and energy. The PA panel shows the current and predicted PV power generation. The OA panel shows the optimized temperature setpoint. This user interface helps the user or operator to monitor the MAS effectively. In addition, the historical data menu provides a feature to download the historical data in comma separated values (CSV) for further analysis, as discussed in the next section.

3.2. PV power prediction accuracy. Table 8 shows the PV power prediction error for four methods. In each method, the root mean square error (RMSE) and mean absolute error (MAE) of the predicted PV power are calculated. The average RMSE and MAE are 198.18 W and 94.60 W, respectively. Observing the maximum value of PV power of 2,692 W, the RMSE and MAE are 7.3% and 3.5% of the maximum PV power, respectively. Fortunately, these values are small and allowable in this application. These results show that the proposed LSTM achieves high accuracy in PV power prediction.

TABLE 8. PV power prediction error

Method	RMSE	MAE
1. No Control	166.54 W	79.20 W
2. Temperature Control	214.51 W	100.83 W
3. Occupancy Control	178.83 W	85.56 W
4. Occupancy and Temperature Control	232.84 W	112.79 W
Average	198.18 W	94.60 W

Figure 5 shows the PV power profiles over five days. The solid red line represents the actual value, while the dashed blue line represents the predicted value. The profiles show that the peak power occurs almost the same at noon every day. However, the morning and afternoon profiles differ on the different days. The figure shows a small discrepancy between the predicted and actual values. Thus, the predicted values can be adopted to evaluate the proposed system because the predicted profile represents the actual PV power generation profile.

In addition, it is interesting to analyze the RMSE and MAE values. The MAE is lower than the RMSE, about half the RMSE. As observed in Figure 5, large errors occur at the

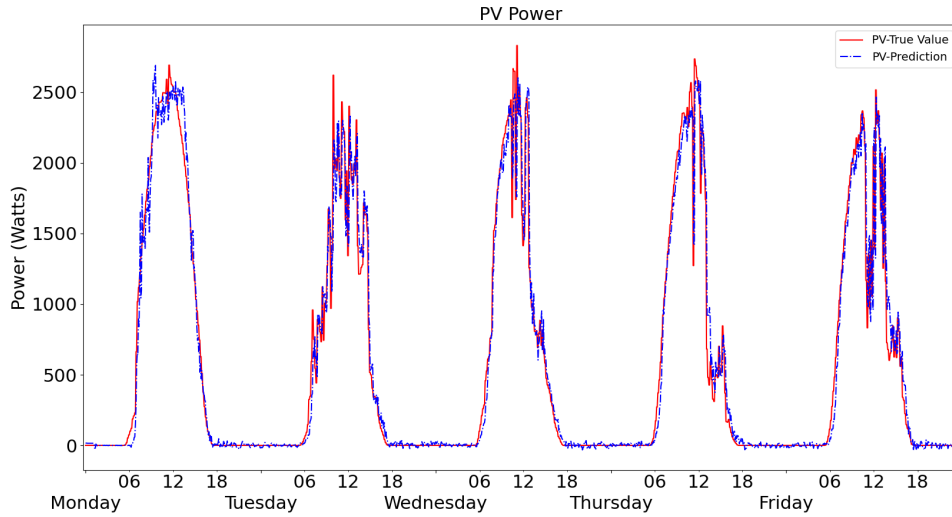


FIGURE 5. PV power prediction

peaks of the PV profile. Since the RMSE tends to give more weight to the more significant errors, the RMSE value is higher than the MAE.

3.3. Energy efficiency. Figure 6 shows the result of the optimized temperature setpoint computed by the MOGA. The figure shows that the current temperature (outdoor temperature) fluctuates from 22°C to 38°C . Since the optimization algorithm described in Equations (1) to (14) optimizes the temperature from 20°C to 24°C , the optimized temperature falls in this range, as shown in the figure. The figure also shows that the optimized temperature tends to reach 24°C in the daytime. This is because the optimization objective is to minimize energy consumption while maintaining user comfort. Thus, when the load power consumption is high in the daytime, the optimized temperature will be achieved at the minimum temperature comfort, i.e., 24°C .

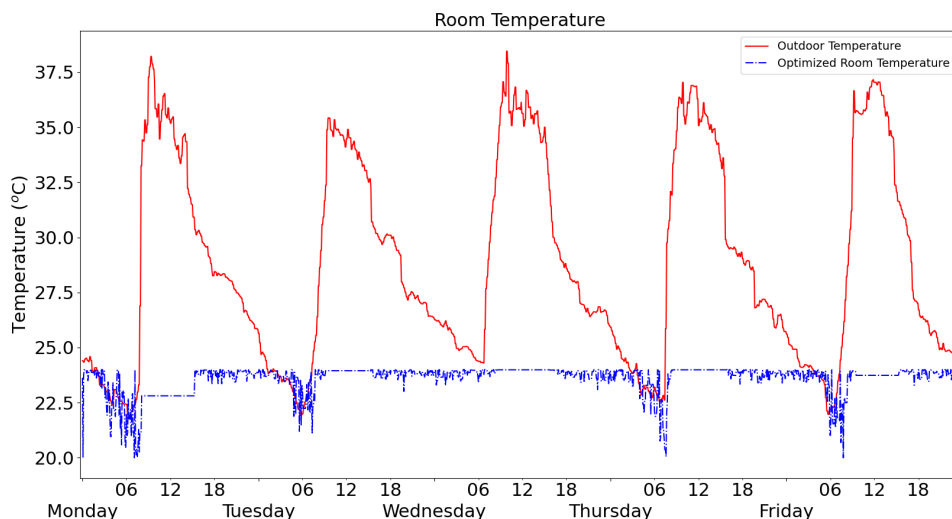


FIGURE 6. Temperature setpoint optimization

Figure 7 shows the five-day lighting power consumption profiles for No Control (red solid line) and Occupancy Control (blue dashed line). The figure clearly shows that Occupancy Control provides better power management, where the lighting power consumption follows

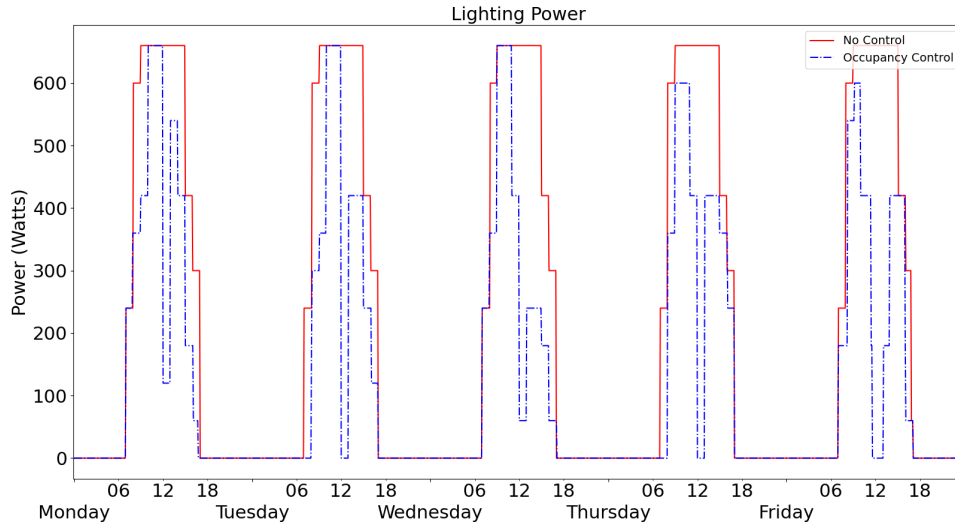


FIGURE 7. Lighting power consumption

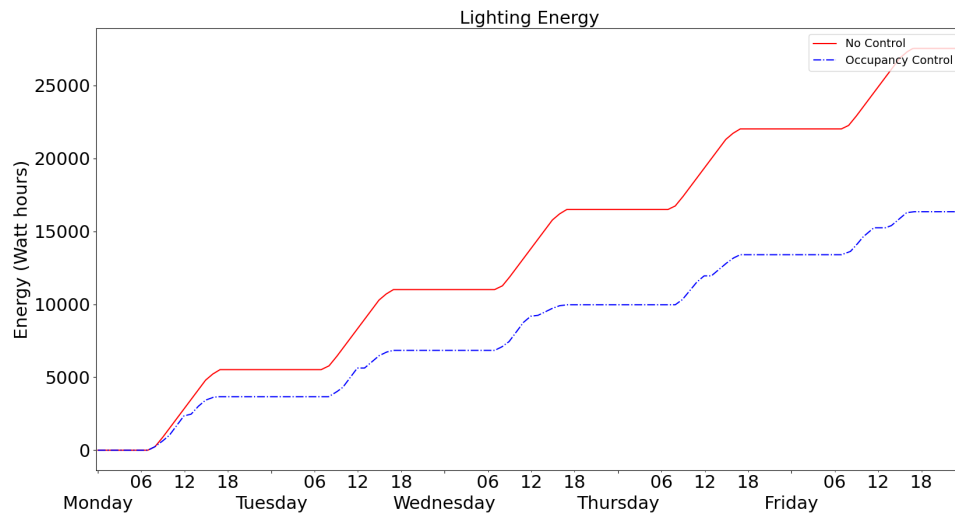


FIGURE 8. Lighting energy consumption

the occupancy status. The respective energy consumption is shown in Figure 8. The figure shows that Occupancy Control can significantly reduce energy consumption.

Figure 9 shows the AC power consumption profiles during five days for No Control (red solid line), Temperature Control (green dashed line), Occupancy Control (blue dash-dotted line), and Occupancy and Temperature Control (black dotted line). The figure clearly shows that Occupancy and Temperature Control achieves the lowest power consumption, followed by Occupancy Control, Temperature Control, and No Control. The AC energy consumption profiles shown in Figure 10 show the same pattern.

To evaluate the effectiveness of the proposed algorithm, the energy consumption reduction of the total energy, AC and lighting energy, and room energy are calculated as given in Tables 9, 10, and 11, respectively. It is noted here that the energy consumption reduction is calculated using the No Control method as the reference.

Observing the total energy consumption reduction in Table 9, the Occupancy and Temperature Control achieves the highest reduction by 40.29%. The Occupancy Control achieves a higher reduction of 32.76% compared to the Temperature Control, which

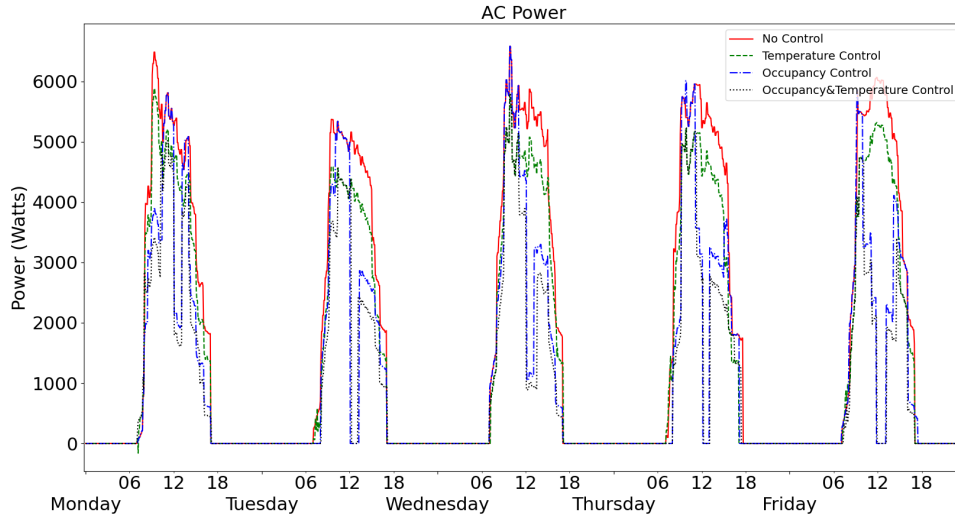


FIGURE 9. AC power consumption

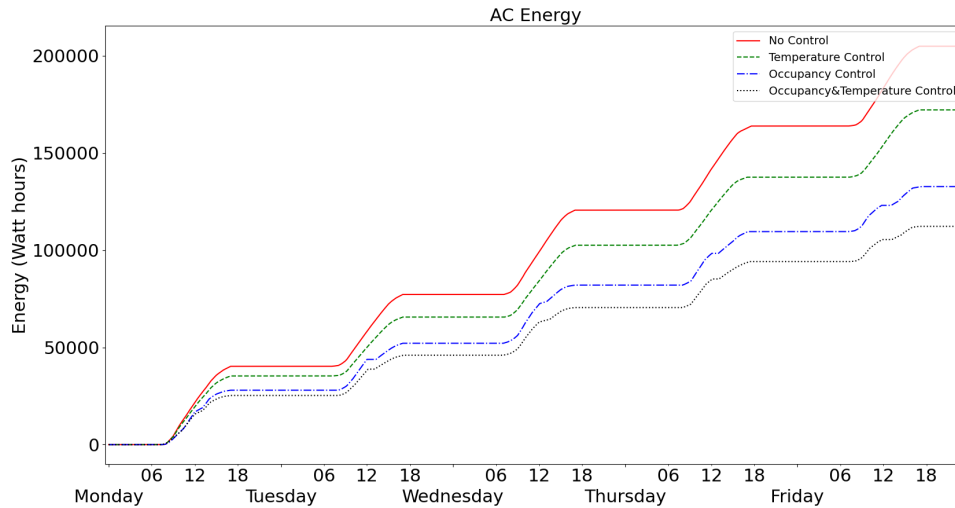


FIGURE 10. AC energy consumption

TABLE 9. Total energy consumption reduction

Method	Energy consumption (Watt hours)					Total energy reduction
	AC	LCD projector	Lighting	Power outlet	Total load	
No Control	204,952	12,000	27,600	27,480	272,032	0.00%
Temperature Control	172,188	12,000	27,600	27,480	239,268	12.04%
Occupancy Control	132,760	11,600	16,290	22,260	182,910	32.76%
Occupancy and Temperature Control	112,291	11,600	16,290	22,260	162,441	40.29%

has a reduction of 12.04%. From Table 10, the reduction in AC energy consumption in Occupancy and Temperature Control is 45.21%, which is higher than the reduction in lighting energy consumption by 40.98%. The results are clearly understood from the fact that AC energy consumption is affected by the temperature and occupancy, while lighting consumption is not affected by the temperature. Table 10 also provides a good insight

TABLE 10. AC and lighting energy consumption reduction

Method	AC		Lighting	
	Energy consumption (Watt hours)	Energy reduction	Energy consumption (Watt hours)	Energy reduction
No Control	204,952	0.00%	27,600	0.00%
Temperature Control	172,188	15.99%	27,600	0.00%
Occupancy Control	132,760	35.22%	16,290	40.98%
Occupancy and Temperature Control	112,291	45.21%	16,290	40.98%

TABLE 11. Classroom, office room, and laboratory room energy consumption reduction

Method	Classroom		Office room		Laboratory room	
	Energy consumption (Watt hours)	Energy reduction	Energy consumption (Watt hours)	Energy reduction	Energy consumption (Watt hours)	Energy reduction
No Control	111,260	0.00%	49,315	0.00%	111,457	0.00%
Temperature Control	96,688	13.09%	43,822	11.14%	98,758	11.39%
Occupancy Control	59,861	46.19%	41,779	15.28%	81,270	27.08%
Occupancy and Temperature Control	52,383	52.91%	36,909	25.16%	73,148	34.37%

into the AC energy consumption efficiency achieved by the Occupancy Control, which is higher than that achieved by the Temperature Control only.

Table 11 shows the energy consumption reduction in the classroom, office, and laboratory. The highest energy reduction of 52.91% is achieved in the classroom using the Occupancy and Temperature Control method, followed by the laboratory and office. This information provides the campus manager with a better understanding of the energy reduction in each room or building.

3.4. Practical implementation performance. In the experiments, the data delivery ratio (DDR) and the execution time of the proposed system are calculated. The DDR is the ratio of the SMA's and OA's received data with the number of data transmitted by the other three agents (TLA, OLA, and PSA). Tables 12 and 13 give the DDR in the SCADA HMI (SMA) and Raspberry Pi (OA), respectively. The tables show that the DDR in SCADA HMI and Raspberry Pi is 94.52% and 93.61%, respectively. It means that a few pieces of data are lost during transmission. The transmission loss can be caused by the MQTT protocol that employs the broker as an intermediate unit for data exchange. In the experiments, since all agents or devices use the same broker, i.e., the Raspberry Pi, and the Raspberry Pi also run several tasks such as generating the simulation data, predicting PV power, and optimizing the temperature setpoints, the Raspberry becomes busy, leading to transmission loss in the MQTT protocol.

Table 14 gives the execution time of the prediction and optimization algorithms. The LSTM training and testing times are 0.4 s and 0.1 s, respectively. This is fast enough

TABLE 12. Data delivery ratio in SCADA HMI

Method	Data delivery ratio (DDR)		
	Temperature-based Load Control Agent (TLA)	Occupancy-based Load Control Agent (OLA)	Power Source Agent (PSA)
No Control	98.75%	97.92%	98.06%
Temperature Control	97.92%	94.79%	98.75%
Occupancy Control	95.07%	85.63%	97.08%
Occupancy and Temperature Control	97.50%	82.43%	90.35%
Average	97.31%	90.19%	96.06%
Total average	94.52%		

TABLE 13. Data delivery ratio in Raspberry Pi

Method	Data delivery ratio (DDR)		
	Temperature-based Load Control Agent (TLA)	Occupancy-based Load Control Agent (OLA)	Power Source Agent (PSA)
No Control	98.19%	69.86%	98.13%
Temperature Control	97.50%	94.38%	98.82%
Occupancy Control	94.72%	89.65%	92.97%
Occupancy and Temperature Control	98.26%	95.76%	90.76%
Average	97.17%	87.41%	96.25%
Total average	93.61%		

TABLE 14. Execution time of prediction and optimization algorithms

Parameter	Value	Note
LSTM training time	0.4 s	Number of neurons = 100 Sequence length = 6 Epoch = 1
LSTM test time	0.1 s	
MOGA execution time	1.3 s	Number of population = 100 Number of iteration = 5,000

compared to the time interval used in this experiment, which is 4 s. The MOGA execution time is 1.3 s, which is still lower than the simulation time interval.

Based on the evaluation described previously, the reliability and safety of the implementation of the proposed testbed in the actual building are discussed in the following. The reliability and safety are described in terms of implementing the EMS algorithms and data communication. The reliability of a system to predict the PV power can be examined from the prediction error in Table 8, wherein each running/simulation period, the error prediction defined by the RMSE is below 240 W (9% from maximum value), and MAE is below 120 W (4% of maximum value). The reliability of the proposed optimization can be observed from the energy consumption reduction in Tables 9, 10, and 11, wherein each table shows that the Temperature Control (optimization algorithm) consistently achieves a higher energy reduction compared to no Temperature Control. The results show that

the proposed system is reliable in making PV power predictions and temperature optimization. Fortunately, these algorithms can be executed fast on the embedded platform, as given in Table 14. Therefore, they are suitable for real-time application in the actual building implementation.

The reliability of data communication can be examined from the DDR given in Tables 12 and 13, where the DDR is about 94%. It means that the reliability of the data communication needs to be higher. As discussed previously, it is caused by implementing many agents on a single Raspberry Pi. It is worth noting that this arrangement is for simplicity during simulation only. In the actual implementation, each agent is implemented on a separate embedded system. Thus, the data communication loss due to the overload of the MQTT broker unit can be minimized.

The safety of the proposed system regarding the experimental testbed can be evaluated by considering several aspects, such as prediction and optimization failures, data communication loss, and slow processing time. The PV power prediction is used as input for the optimization process. Thus, the prediction failure will cause the wrong or failure in the optimization output, i.e., the optimized room temperature setpoint. Fortunately, since the temperature setpoint of the AC is limited by a particular allowable range, the optimization failure does not cause the AC operation to malfunction. In the proposed system architecture, the loss of data communication will affect the rooms' Temperature and Occupancy Control. The effect of data communication loss in Temperature Control is similar to the optimization failure discussed previously. The data communication loss causes the Occupancy Control not to work. Thus, the system will work without a control method and energy consumption reduction. However, there was no malfunction in the load operation in the room. Therefore, it is suggested that local control redundancy be adopted. From the discussion, it can be concluded that the proposed system provides safety for the actual implementation.

3.5. Comparison to existing works. Table 15 compares the existing works. It compares several parameters, such as the implementation platform, prediction technique, optimization technique, real-time processing, and user interface agent feature. These parameters are selected to evaluate the reliability of a real-time implementation. Based on the comparison in Table 15, our proposed system shows superiority in that all five parameters are complied. More specifically, our approach provides the prediction technique and

TABLE 15. Comparison to existing works

	Implementation	Prediction	Optimization	Real-time	User interface agent
[25]	Raspberry Pi	No	Decision making	Yes	Django framework
[27]	Raspberry Pi	No	GA	Yes	No
[28]	Simulation software	No	PSO	No	No
[30]	Simulation software	No	Case-based reasoning	No	No
[31]	MATLAB	ANN*	ANN*	No	MATLAB
[32]	Raspberry Pi	No	Rule-based	Yes	Web service
Proposed	Raspberry Pi	LSTM	GA	Yes	HMI SCADA

*: ANN is used to predict the optimized set values.

introduces the SCADA system as the user interface agent for a better energy management system.

4. Conclusions. An experimental MAS-based campus energy management system testbed was developed using the embedded platform and SCADA system. The proposed approach combines the prediction and optimization techniques for efficient implementation in real-time applications. It uses embedded devices' benefits for implementation, the LSTM-based PV power prediction and GA-based optimization, and the established SCADA monitoring system. The proposed testbed was tested for optimizing the energy consumption in the campus building consisting of the classroom, office room, and laboratory room, which the grid-connected PV powers. The experimental results show promising results for the real-time implementation of an efficient BEMS.

The proposed system will be extended to cope with the complex BEMS involving advanced architecture. For example, it will adopt multi-communication protocols, namely Zigbee, WiFi, and LoRa, to cover many classrooms in the large campus building, integrating and extending to the smart classroom and smart campus. The prediction algorithm will be extended for room temperature and load prediction. The optimization algorithm will be improved by investigating other AI-based optimization techniques. Furthermore, implementation will be carried out in the actual campus building.

Acknowledgment. This work was supported by a Research Grant from the Ministry of Education, Culture, Research, and Technology, Republic of Indonesia, 2024 (No.: SP DIPA-023.17.1.690523/2024).

REFERENCES

- [1] U. Mir, U. Abbasi, T. Mir, S. Kanwal and S. Alamri, Energy management in smart buildings and homes: Current approaches, a hypothetical solution, and open issues and challenges, *IEEE Access*, vol.9, pp.94132-94148, DOI: 10.1109/ACCESS.2021.3092304, 2021.
- [2] S. Mischos, E. Dalagdi and D. Vrakas, Intelligent energy management systems: A review, *Artif. Intell. Rev.*, vol.56, no.10, pp.11635-11674, DOI: 10.1007/s10462-023-10441-3, 2023.
- [3] U. K. Seng, H. Malik, F. P. García Márquez, M. A. Alotaibi and A. Afthanorhan, Fuzzy logic-based intelligent energy management framework for hybrid PV-wind-battery system: A case study of commercial building in Malaysia, *J. Energy Storage*, vol.102, no.10, DOI: 10.1016/j.est.2024.114109, 2024.
- [4] A. El Zerk and M. Ouassaid, Real-time fuzzy logic based energy management system for microgrid using hardware in the loop, *Energies*, vol.16, no.5, DOI: 10.3390/en16052244, 2023.
- [5] E. Giglio, G. Luzzani, V. Terranova, G. Trivigno, A. Niccolai and F. Grimaccia, An efficient artificial intelligence energy management system for urban building integrating photovoltaic and storage, *IEEE Access*, vol.11, no.2, pp.18673-18688, DOI: 10.1109/ACCESS.2023.3247636, 2023.
- [6] O. Ibrahim et al., Development of fuzzy logic-based demand-side energy management system for hybrid energy sources, *Energy Convers. Manag. X*, vol.18, no.1, DOI: 10.1016/j.ecmx.2023.100354, 2023.
- [7] N. A. Mahmud, N. Y. Dahlan, W. N. W. M. Adnan, A. Tumian and M. S. Onn, Optimum energy management strategy with NEM-ETOU for campus buildings installed with solar PV using EPSO, *Energy Reports*, vol.9, no.9, pp.54-59, DOI: 10.1016/j.egy.2023.09.124, 2023.
- [8] X. Xing and L. Jia, Energy management in microgrid and multi-microgrid, *IET Renew. Power Gener.*, no.1, DOI: 10.1049/rpg2.12816, 2023.
- [9] H. Zhang, S. Seal, D. Wu, F. Bouffard and B. Boulet, Building energy management with reinforcement learning and model predictive control: A survey, *IEEE Access*, vol.10, pp.27853-27862, DOI: 10.1109/ACCESS.2022.3156581, 2022.
- [10] A. Soetedjo, Y. I. Nakhoda and C. Saleh, Embedded fuzzy logic controller and wireless communication for home energy management systems, *Electron.*, vol.7, no.9, DOI: 10.3390/electronics7090189, 2018.

- [11] D. Kontogiannis, D. Bargiotas and A. Daskalopulu, Fuzzy control system for smart energy management in residential buildings based on environmental data, *Energies*, vol.14, no.3, DOI: 10.3390/en14030752, 2021.
- [12] R. O. Ibrahim, E. Tambo, D. Tsuanyo and A. Nguedia-Nguedoung, Modelling an artificial intelligence-based energy management for household in Nigeria, *Eng. Lett.*, vol.30, no.1, pp.140-151, 2022.
- [13] H. V. V. Priyadarshana, M. A. K. Sandaru, K. T. M. U. Hemapala and W. D. A. S. Wijayapala, A review on multi-agent system based energy management systems for micro grids, *AIMS Energy*, vol.7, no.6, pp.924-943, DOI: 10.3934/ENERGY.2019.6.924, 2019.
- [14] O. P. Mahela et al., Comprehensive overview of multi-agent systems for controlling smart grids, *CSEE J. Power Energy Syst.*, vol.8, no.1, pp.115-131, DOI: 10.17775/CSEEJPES.2020.03390, 2022.
- [15] W. Wei and J. Lv, Multi-agent event-triggered containment control with joint connected switching topology, *International Journal of Innovative Computing, Information and Control*, vol.18, no.3, pp.957-971, DOI: 10.24507/ijicic.18.03.957, 2022.
- [16] E. Samadi, A. Badri and R. Ebrahimpour, Decentralized multi-agent based energy management of microgrid using reinforcement learning, *Int. J. Electr. Power Energy Syst.*, vol.122, no.2, 106211, DOI: 10.1016/j.ijepes.2020.106211, 2020.
- [17] A. A. Abdelsalam, H. A. Zedan and A. A. ElDesouky, Energy management of microgrids using load shifting and multi-agent system, *J. Control. Autom. Electr. Syst.*, vol.31, no.4, pp.1015-1036, DOI: 10.1007/s40313-020-00593-w, 2020.
- [18] S. S. Binyamin and S. B. Slama, Multi-agent systems for resource allocation and scheduling in a smart grid, *Sensors*, vol.22, no.21, DOI: 10.3390/s22218099, 2022.
- [19] Z. Vale, P. Faria, O. Abrishambaf, L. Gomes and T. Pinto, MARTINE – A platform for real-time energy management in smart grids, *Energies*, vol.14, no.7, pp.1-14, DOI: 10.3390/en14071820, 2021.
- [20] Y. AL Sultan, B. S. Sami and B. A. Zafar, Smart home energy management system: A multi-agent approach for scheduling and controlling household appliances, *Int. J. Adv. Comput. Sci. Appl.*, vol.12, no.3, pp.237-244, DOI: 10.14569/IJACSA.2021.0120329, 2021.
- [21] S. Gherairi, Design and implementation of an intelligent energy management system for smart home utilizing a multi-agent system, *Ain Shams Eng. J.*, vol.14, no.3, DOI: 10.1016/j.asej.2022.101897, 2023.
- [22] X. Xu, Y. Jia, Y. Xu, Z. Xu, S. Chai and C. S. Lai, A multi-agent reinforcement learning-based data-driven method for home energy management, *IEEE Trans. Smart Grid*, vol.11, no.4, pp.3201-3211, DOI: 10.1109/TSG.2020.2971427, 2020.
- [23] J. Lu, P. Mannion and K. Mason, A multi-objective multi-agent deep reinforcement learning approach to residential appliance scheduling, *IET Smart Grid*, vol.5, no.4, pp.260-280, DOI: 10.1049/stg2.12068, 2022.
- [24] M. Hall and A. Geissler, Load control by demand side management to support grid stability in building clusters, *Energies*, vol.13, no.19, DOI: 10.3390/en13195112, 2020.
- [25] Z. Boussaada et al., Multi agent architecture for smart building energy management, *2020 6th IEEE Congress on Information Science and Technology (CiSt)*, pp.455-460, 2021.
- [26] A. Soetedjo, Y. I. Nakhoda and C. Saleh, Intelligent multi agent system for energy management in the classrooms with grid connected PV, *Proc. of 2019 IEEE International Conference on Mechatronics and Automation (ICMA 2019)*, DOI: 10.1109/ICMA.2019.8816347, 2019.
- [27] A. Soetedjo, Y. I. Nakhoda and C. Saleh, An embedded platform for testbed implementation of multi-agent system in building energy management system, *Energies*, vol.12, no.19, DOI: 10.3390/en12193655, 2019.
- [28] S. S. Ghazimirsaeid, M. S. Jonban, M. W. Mudiyansele, M. Marzband, J. L. R. Martinez and A. Abusorrah, Multi-agent-based energy management of multiple grid-connected green buildings, *J. Build. Eng.*, vol.74, no.5, DOI: 10.1016/j.jobbe.2023.106866, 2023.
- [29] K. Nweye, B. Liu, P. Stone and Z. Nagy, Real-world challenges for multi-agent reinforcement learning in grid-interactive buildings, *Energy AI*, vol.10, no.9, 2022.
- [30] T. Pinto, R. Faia, M. Navarro-Caceres, G. Santos, J. M. Corchado and Z. Vale, Multi-agent-based CBR recommender system for intelligent energy management in buildings, *IEEE Syst. J.*, vol.13, no.1, pp.1084-1095, DOI: 10.1109/JSYST.2018.2876933, 2019.
- [31] A. Verma, S. Prakash and A. Kumar, AI-based building management and information system with multi-agent topology for an energy-efficient building: Towards occupants comfort, *IETE J. Res.*, vol.69, no.2, pp.1033-1044, DOI: 10.1080/03772063.2020.1847701, 2023.

- [32] U. Na and E. K. Lee, Fog BEMS: An agent-based hierarchical fog layer architecture for improving scalability in a building energy management system, *Sustain.*, vol.12, no.7, pp.1-28, DOI: 10.3390/su12072831, 2020.
- [33] S. Taheri, A. J. Amiri and A. Razban, Real-world implementation of a cloud-based MPC for HVAC control in educational buildings, *Energy Convers. Manag.*, vol.305, no.2, DOI: 10.1016/j.enconman.2024.118270, 2024.
- [34] S. van Roosmale, P. Hellinckx, J. Meysman, S. Verbeke and A. Audenaert, Building automation and control systems for office buildings: Technical insights for effective facility management – A literature review, *J. Build. Eng.*, vol.97, no.10, pp.1-16, DOI: 10.1016/j.jobbe.2024.110943, 2024.
- [35] Um-e-Habiba, I. Ahmed, M. Asif, H. H. Alhelou and M. Khalid, A review on enhancing energy efficiency and adaptability through system integration for smart buildings, *J. Build. Eng.*, vol.89, no.4, DOI: 10.1016/j.jobbe.2024.109354, 2024.
- [36] K. H. Yu et al., Optimization of thermal comfort, indoor quality, and energy-saving in campus classroom through deep Q learning, *Case Stud. Therm. Eng.*, vol.24, no.1, DOI: 10.1016/j.csite.2021.100842, 2021.
- [37] *OpenMQTTGateway v1.7.0*, <https://docs.openmqttgateway.com/>, Accessed on Jul. 01, 2024.
- [38] *Platypus*, <https://github.com/Project-Platypus/Platypus>, Accessed on Jul. 01, 2024.
- [39] D. K. Dhaked, S. Dadhich and D. Birla, Power output forecasting of solar photovoltaic plant using LSTM, *Green Energy Intell. Transp.*, vol.2, no.5, DOI: 10.1016/j.geits.2023.100113, 2023.
- [40] M. S. Hossain and H. Mahmood, Short-term photovoltaic power forecasting using an LSTM neural network and synthetic weather forecast, *IEEE Access*, vol.8, pp.172524-172533, DOI: 10.1109/ACCESS.2020.3024901, 2020.
- [41] H. Chen and X. Chang, Photovoltaic power prediction of LSTM model based on Pearson feature selection, *Energy Reports*, vol.7, pp.1047-1054, DOI: 10.1016/j.egy.2021.09.167, 2021.

Author Biography



Aryuanto Soetedjo received the B.Eng. and M.Eng. degrees in Electrical Engineering from Bandung Institute of Technology, Indonesia, in 1993 and 2002, respectively, and the Dr. Eng. degree in Information Science and Control Engineering from Nagaoka University of Technology, Japan, in 2006.

He is currently a full-time professor at the Department of Electrical Engineering, National Institute of Technology (ITN) Malang, Indonesia. His main research interests are image processing, artificial intelligence, machine learning, Internet of Things, control system, and robotics.



Irrine Budi Sulistiawati received a Doctoral degree in 2016 at the Institut Teknologi Sepuluh Nopember (ITS) Surabaya.

She is currently an associate professor at the Department of Electrical Engineering, National Institute of Technology (ITN) Malang, Indonesia. Her main research interests are the stability of electric power systems, particularly transient stability. She is also active in research related to energy management and technology-related renewable energy.



Radimas Putra Muhammad Davi Labib received a Bachelor degree in Electrical Engineering at National Institute of Technology (ITN) Malang in 2016 and a Master degree in Electrical Engineering at Institut Teknologi Sepuluh Nopember, Surabaya in 2019.

He currently works as a lecturer in Department of Electrical Engineering at the Faculty of Industrial Technology at National Institute of Technology (ITN) Malang, Indonesia. His research interests include robotics, optimization, artificial intelligence, machine learning, and computer vision.